

# RADIATION EFFECT ON MHD STAGNATION-POINT FLOW AND MELTING HEAT TRANSFER OF MICROPOLAR NANOFLUID OVER A LINEAR STRETCHING SHEET

B.J.Gireesha<sup>a\*</sup>, M.R.Krishnamurthy<sup>b</sup>, B.C.Prasannakumara<sup>c</sup>, N.G.Rudraswamy<sup>d</sup>, K.Ganeshkumar<sup>a</sup> and M.Umeshaiah<sup>e</sup>

<sup>a</sup>Department of Studies and Research in Mathematics, Kuvempu University,  
Shankaraghatta-577 451, Shimoga, Karnataka, INDIA.

<sup>b</sup>Department of Mathematics, JNNCE Shimoga-577201, Karnataka, INDIA

<sup>c</sup>Department of Mathematics, Government First Grade College, Koppa,  
Chikkamagaluru-577126, Karnataka, INDIA.

<sup>d</sup>Department of Mathematics, Sahyadri Science College,  
Shimoga-577201, Karnataka, INDIA.

<sup>e</sup>Department of Mathematics, PESTIM College, Shimoga-577201, Karnataka, INDIA.

E-mail: [bjgireesu@gmail.com](mailto:bjgireesu@gmail.com), [krishnamaths268@gmail.com](mailto:krishnamaths268@gmail.com), [dr.bcprasanna@gmail.com](mailto:dr.bcprasanna@gmail.com), [ngrudraswamy@gmail.com](mailto:ngrudraswamy@gmail.com), [ganikganesh@gmail.com](mailto:ganikganesh@gmail.com) and [umeshaiah1979@gmail.com](mailto:umeshaiah1979@gmail.com)

---

**Abstract:** This article investigates the radiation effects on the steady MHD boundary layer stagnation-point flow of a micropolar fluid towards a horizontal linearly stretching sheet in the presence of nanoparticles. A mathematical model is developed to study the heat transfer characteristics occurring during the melting process due to a stretching sheet. Suitable similarity transformations are employed to reduce the governing partial differential equations into the system of ordinary differential equations. The transformed non-linear ordinary differential equations governing the flow are solved numerically by the Runge-Kutta-Fehlberg-45 method with Shooting technique. Results for the velocity, temperature and concentration distributions are presented graphically for different values of the pertinent parameters.

**Key Words:** Boundary layer flow, nanofluid, stretching sheet, melting heat transfer, stagnation point flow, thermal radiation.

## 1. Introduction

The boundary layer flow of non-Newtonian fluids has attracted a large class of applications in engineering practice, particularly in applied geophysics, geology, groundwater flow and oil reservoir engineering. In recent years, a great deal of interest has been generated in the area of two dimensional boundary-layer flow over a stretching surface near a stagnation-point in view of its numerous and wide range of applications in various technical and industrial fields such as cooling of electronic devices by fans, cooling of nuclear reactors during emergency shutdown, heat exchangers placed in a low-velocity environment, solar central receivers exposed to wind currents, and many hydrodynamic processes. Stagnation-point flow, describing the fluid motion near the stagnation region of a circular body, exists for both the cases of a fixed or moving body in a fluid. The stagnation region encounters the highest pressure, the heat transfer, and the rate of mass deposition. The two-dimensional flow of a fluid near a stagnation point was first examined by Hiemenz [1]. Later, the prob-

lem of stagnation point flow was extended to various Newtonian/non-Newtonian fluids with various physical effects and different thermal boundary conditions. Following the pioneer work by Yang [2], the problem was extended to unsteady axis-symmetric stagnation-point flow by Williams III [3] and to a general three dimensional stagnation-point flow by Jankowski and Gersting [4]. Very recently, Awaludin et al. [5] considered the stability analysis of stagnation point flow over a linearly stretching or shrinking sheet. Zaimi and Ishak [6] examined the effects of partial slip on stagnation-point flow and heat transfer due to a stretching vertical sheet.

---

\*Corresponding Author, Email: [bjgireesu@gmail.com](mailto:bjgireesu@gmail.com)

Over the last few years a considerable amount of experimental and numerical research has been

carried out to determine the role of natural convection in the kinetics of heat transfer accompanied with melting or solidification effect. Processes involving melting heat

transfer in non-Newtonian fluids have promising applications in thermal engineering such as oil extraction, magma solidification, melting of permafrost, geothermal energy recovery, silicon wafer process, thermal insulation, etc. Roberts [7] was the first to describe the melting phenomena of ice placed in a hot stream of air at a steady state. Epstein and Cho [8] studied, laminar film condensation on a vertical melting surface. Chamkha et al. [9] analyzed hydromagnetic, forced convection, boundary-layer flow with heat and mass transfer of a nanofluid over a horizontal stretching plate in the presence of a transverse magnetic field, melting and heat generation or absorption effects. Abel and Jayashree Sanamani [10] carried out to study the steady two-dimensional stagnation-point flow and heat transfer from a warm, laminar liquid flow to a melting stretching sheet.

The theory of micropolar fluids takes into account the microscopical effects arising from the local microstructure and intrinsic motion of the fluid elements, and is expected to provide a mathematical model for non-Newtonian fluid behavior. Theory of micropolar fluids was first proposed by Eringen [11]. Bachok et al. [12] studied the effect of melting heat transfer in boundary layer stagnation-point flow towards a stretching/shrinking sheet. Yacob et al. [13] investigated the boundary layer stagnation-point flow and heat transfer over a stretching/shrinking sheet immersed in a micropolar fluid in the presence of melting effect. Ishak et al. [14] obtained Dual solutions in mixed convection boundary layer flow of micropolar flow and heat transfer characteristics of micropolar fluid in the melting process towards a porous stretching/shrinking surface. Recently, Mohanty et al. [16] presented the study of unsteady heat and mass transfer characteristics of a viscous incompressible electrically conducting micropolar fluid.

A Nanofluid is a fluid containing nanometer-sized particles, called nanoparticles. These fluids are engineered colloidal suspensions of nanoparticles in a base fluid. The nanoparticles used in nanofluids are typically made of metals, oxides, carbides, or carbon nanotubes. Buongiorno [17] proposed a model for nanofluid. Goyal and Bhargava [18] theoretically investigated the conjugate effects of viscous dissipation and non-uniform heat source/sink on the double-diffusive boundary layer flow of a viscoelastic nanofluid over a stretching sheet. Khan and Gorla [19] studied heat and mass transfer in non-Newtonian nanofluids over a stretching surface with prescribed wall temperature and surface nanoparticle concentration. The Buongiorno and Darcy models have been used by Khan et al [20] to investigate the effects of momentum slip on the double-diffusive free convective flow past a convectively heated vertical plate in a medium saturated with nanofluids. Kuznetsov and Nield [21] is the first who considered the problem on stretching sheet in nanofluids. Gorla et al [22] studied the effect of melting on heat transfer in a nanofluid flow past a permeable continuous moving surface. The model proposed by Tiwari and Das [23], is different from the above and which was also used by several authors ( Abu-Nada [24], Muthamilselvan et al. [25], Talebi et al. [26], Ahmad et al. [27], Bachok et al. [28, 29], Yacob et al. [30]). Buongiorno [17] studies the Brownian

motion and the thermophoresis on the heat transfer characteristics with his model, while the model proposed by Tiwari and Das [23] analyzes the behavior of nanofluids taking into account the solid volume fraction. Mabood and Das [31] presented the MHD flow and melting heat transfer of a nanofluid over a stretching surface taking into account a second-order slip model and thermal radiation. Hayat et al. [32] concentrated on the mathematical modeling for stagnation point flow and melting heat transfer of nanofluids over an impermeable stretching sheet with variable thickness.

In the recent year, non-Newtonian fluids have become more and more important due to its industrial applications. Many studies are focused on non-Newtonian fluid as a base fluid with suspended nanoparticles over a stretching sheet. Rizwan et al. [33] presented the nanoparticles analysis for the Casson fluid model assuming the convective surface boundary conditions. Malik et al. [34] obtained the similarity solution for a steady boundary layer flow and heat transfer of a Casson nanofluid over a vertical cylinder which is stretching exponentially along its radial direction. Jeffrey fluid has ability to exhibit the properties of ratio of stress relaxation to retardation and retardation. The steady flow of a Jeffrey fluid model in the presence of nano particles is studied by Nadeem et al. [35]. Shehzad et al. [36] developed a solar energy model to explore the characteristics of thermophoresis and Brownian motion in magnetohydrodynamic three-dimensional flow of nano Jeffrey fluid. In another investigation, Nadeem et al. [37] have examined a steady stagnation point flow of Jeffrey nanofluid over an exponential stretching surface under the boundary layer assumptions. Shehzad et al. [38] studied the influence of nanoparticles in MHD flow of Jeffrey fluid over a stretched surface. They considered the thermal and nanoparticles concentration convective boundary conditions. Hussain et al. [39] carried out an analysis to discuss Heat and mass transfer analysis of two-dimensional hydromagnetic flow of an incompressible Jeffrey nanofluid over an exponentially stretching surface. Khan et al. [40] analyzed the free convective boundary-layer flow of three-dimensional Oldroyd-B nanofluid flow over a bi-directional stretching sheet with heat generation/absorption. They employed Oldroyd-B fluid model to describe rheological behavior of visco-elastic nanofluid. Hayat et al. [41] obtained series solution using a well-known analytic approach homotopy analysis method (HAM) for the flow of visco-elastic nanofluid over a stretching cylinder with simultaneous effects of heat and mass transfer. Nadeem and Hussain [42] discussed the two-dimensional flow of Williamson fluid over a stretching-sheet under the effects of nano-sized particle also described as nano Williamson fluid. Recently, Ramesh and Gireesha [43] reported heat source/sink effects on the steady boundary layer flow of a Maxwell fluid over a stretching sheet with convective boundary condition in the presence of nanoparticles. Hayat and Farooq [44] examined the stagnation point flow and melting heat transfer of Maxwell fluid over a stretching sheet with double-diffusive convection. Recently, Krishnamurthy et al. [45] investigated the radiation and chemical reaction effects on the

steady boundary layer flow and melting heat transfer of MHD Williamson fluid through porous medium toward a horizontal linearly stretching sheet in the presence of nanoparticles.

The objective of the present study is to highlight the influence of melting heat transfer on the stagnation-point flow of a micropolar fluid in presence of Nanoparticle over a stretching sheet in presence of radiation and applied magnetic field. Such an analysis has not been yet reported even for any non-Newtonian nanofluid with or without stagnation-point. In the following sections, boundary layer equations for the flow and heat transfer of a micropolar fluid in the presence of nanoparticles towards a horizontal stretching is given along with boundary conditions. Suitable similarity transformations are employed to reduce the governing partial differential equations into the system of ordinary differential equations. Numerical Procedure and numerical solutions of the equations of motion and heat are given. Detailed development of the flow structure and temperature profiles are presented graphically for different values of the pertinent parameters.

## 2. Mathematical formulation and solution of the problem

Consider a steady boundary layer flow and heat transfer of a micropolar fluid in the presence of nanoparticles towards a horizontal stretching sheet melting at a steady rate into a constant property, warm liquid of the same material. It is assumed that the velocity of the external flow is  $U_e(x) = ax$  and the velocity of the stretching/shrinking sheet is  $U_w(x) = cx$ , where  $a$  is a positive constant, while  $c$  is a positive (stretching sheet) and  $x$  is the coordinate measured along the stretching sheet. It is also assumed that the temperature of the melting surface is  $T_m$ , while the temperature in the free-stream condition is  $T_\infty$ , where  $T_\infty > T_m$ . The viscous dissipation and the heat generation or absorption are assumed to be negligible small.

Under these assumptions, the equations of motion and the equation representing temperature distribution in the Micropolar liquid flow in the presence of nanoparticle must obey the usual boundary layer equations:

$$\frac{\partial u}{\partial x} + \frac{\partial v}{\partial y} = 0, \quad (2.1)$$

$$u \frac{\partial u}{\partial x} + v \frac{\partial u}{\partial y} = \left( \frac{u+N}{\rho} \right) \frac{\partial^2 u}{\partial y^2} + \frac{k}{\rho} \frac{\partial N}{\partial y} + U_e \frac{dU_e}{dx} - \frac{\sigma B_0^2}{\rho} u, \quad (2.2)$$

$$u \frac{\partial N}{\partial x} + v \frac{\partial N}{\partial y} = \frac{\gamma}{\rho j} \frac{\partial^2 N}{\partial y^2} - \frac{k}{\rho j} \left( 2N + \frac{\partial u}{\partial y} \right), \quad (2.3)$$

$$u \frac{\partial T}{\partial x} + v \frac{\partial T}{\partial y} = \alpha_m \frac{\partial^2 T}{\partial y^2} + \tau \left[ D_B \frac{\partial C}{\partial y} \frac{\partial T}{\partial y} + \frac{D_T}{D_m} \left( \frac{\partial T}{\partial y} \right)^2 \right] - \frac{1}{(\rho c)_f} \frac{\partial q_r}{\partial y}, \quad (2.4)$$

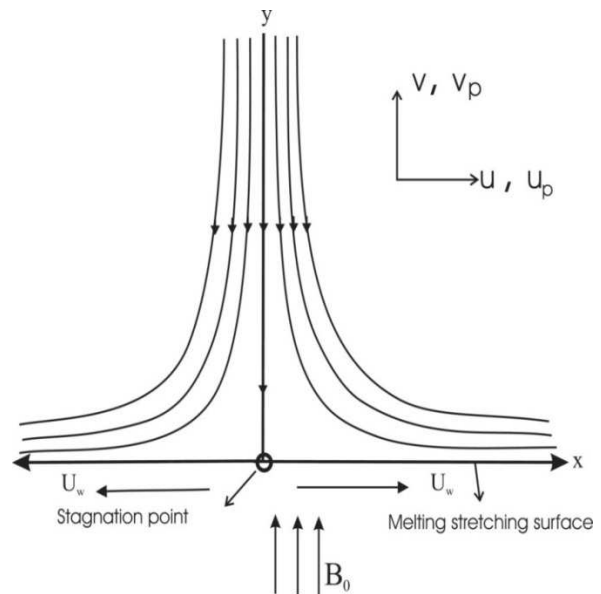


Figure 1: Schematic representation of boundary layer flow.

$$u \frac{\partial C}{\partial x} + v \frac{\partial C}{\partial y} = D_B \frac{\partial^2 C}{\partial y^2} + \frac{D_T}{D_m} \frac{\partial^2 T}{\partial y^2}, \quad (2.5)$$

We assume that the boundary conditions of equations (2.1) – (2.5) are given by,

$$u = U_w(x) = cx, N = -n \frac{\partial u}{\partial y}, T = T_m, C = C_w \text{ at } y = 0, \\ u = U_e(x) = ax, N = 0, T \rightarrow T_\infty, C \rightarrow C_\infty \text{ as } y \rightarrow \infty \text{ and} \quad (2.6)$$

$$k \left( \frac{\partial T}{\partial y} \right)_{y=0} = \rho [\lambda + c_s (T_m - T_0)] v(x, 0). \quad (2.7)$$

Here  $u$  and  $v$  are the velocity components along the  $x$  and  $y$  axes, respectively. Further,  $\mu, K, \rho, T, j, N, \gamma$  and  $\alpha_m$  are respectively the dynamic viscosity, vortex viscosity (or the microrotation viscosity), fluid density, fluid temperature, microinertia density, microrotation (or angular velocity), spin gradient viscosity and nanofluid thermal diffusivity. Further,  $k$  is the thermal conductivity,  $\lambda$  is the latent heat of the fluid and  $c_s$  is the heat capacity of the solid surface. Equation (2.6) states that the heat conducted to the melting surface is equal to the heat of melting plus the sensible heat required to raise the solid temperature  $T_0$  to its melting temperature  $T_m$ . The case  $n = 0$ , is called strong concentration indicates  $N = 0$  near the wall, represents concentrated particle flows in which the microelements close to the wall surface are unable to rotate. The case  $n = \frac{1}{2}$  indicates the vanishing of anti-symmetric part of the stress tensor and denotes weak concentrations. The case  $n = 1$ , is used for the modeling of turbulent boundary layer flows. Further, we follow the work of many recent authors by assuming that  $\gamma = \left( \mu + \frac{k}{2} \right) j = \mu \left( 1 + \frac{R}{2} \right) j$ , where  $R = \frac{k}{\mu}$  is the micropolar or material parameter and  $j = \frac{v_0}{\alpha}$  is a reference length. This assumption is invoked to allow the field of equations predicts the correct behavior in the limiting case

when the microstructure effects become negligible and the total spin  $N$  reduces to the angular velocity.

Using Rosseland approximation for radiation, the radiative heat flux is simplified as,

$$q_r = -\frac{4\sigma^*}{3k^*} \frac{\partial T^4}{\partial y} \quad (2.8)$$

where  $\sigma^*$  and  $k^*$  are the Stefan-Boltzmann constant and the mean absorption coefficient respectively. The temperature differences within the flow are assumed to be sufficiently small so that  $T^4$  may be expressed as a linear function of temperature  $T$  using a truncated Taylor series about the free stream temperature  $T_\infty$  and neglecting the higher order terms, we get,

$$T^4 \approx 4TT_\infty^3 - 3T_\infty^4 \quad (2.9)$$

The momentum, angular momentum, energy equations and concentration equations can be transformed into the corresponding ordinary differential equations by the following similarity variables\

$$\psi = (\alpha\nu)^{\frac{1}{2}} x f(\eta), \quad \eta = \left(\frac{\alpha}{\nu}\right)^{1/2} y, \quad N = x\alpha(\alpha\nu)^{1/2} g(\eta),$$

$$\theta(\eta) = \frac{T-T_m}{T_\infty-T_m}, \quad \phi(\eta) = \frac{c-c_w}{c_\infty-c_w} \quad (2.10)$$

The stream function  $\psi$  is defined such that

$$u = \frac{\partial \psi}{\partial y} \text{ and } v = -\frac{\partial \psi}{\partial x}.$$

The transformed ordinary differential equations are,

$$(1 + R)f'''' + ff'' - (f')^2 + Rg' + 1 - Qf' = 0, \quad (2.11)$$

$$\left(1 + \frac{R}{2}\right)g'' + fg' - f'g - R[2g + f'''] = 0, \quad (2.12)$$

$$\left(\frac{1+N\gamma}{Pr}\right)\theta'' + f\theta' + Nb\phi'\theta' + Nt(\theta')^2 = 0, \quad (2.13)$$

$$\phi'' + Lef\phi' + \frac{Nt}{Nb}\theta'' = 0, \quad (2.14)$$

where a prime denotes differentiation with respect to  $\eta$ ,

$Q = \frac{\sigma\epsilon^2}{\rho\alpha}$  is the magnetic parameter,  $Pr = \frac{\nu}{\alpha_m}$  is the Prandtl

number,  $N\gamma = \frac{16\sigma^*T_\infty^3}{3k^*}$  is the radiation parameter,

$Nb = \frac{\tau D_B (c_\infty - c_w)}{\nu}$  is Brownian motion parameter,

$Nt = \frac{\tau D_T (T_\infty - T_m)}{\nu T_\infty}$  is the thermophoresis parameter and

$Le = \frac{\nu}{D_B}$  is the Lewis number.

The boundary conditions (2.6) become,

$$f'(0) = A, \quad g(0) = -nf''(0), \quad Prf(0) + M\theta'(0) = 0, \quad \theta(0) = 0, \quad \phi(0) = 0,$$

$$f'(\infty) = 1, \quad g(\infty) = 0, \quad \theta(\infty) = 1, \quad \phi(\infty) = 1, \quad (2.15)$$

where  $A = \frac{\epsilon}{\alpha}$  is the stretching ( $\epsilon \geq 0$ ) parameter and  $M$

is the dimensionless melting parameter

which is defined as,

$$M = \frac{c_f(T_\infty - T_m)}{\lambda + c_s(T_m - T_0)} \quad (2.16)$$

which is a combination of the Stefan number  $\frac{c_f(T_\infty - T_m)}{\lambda}$  and  $\frac{c_s(T_m - T_0)}{\lambda}$  for the liquid and solid phases, respectively. It is worth mentioning that for  $M = 0$  (melting is absent) and  $R = 0$  (viscous fluid) the problem reduces to that considered by Wang [46].

### 3. Numerical Procedure

The non-linear ordinary differential equations (2.11)-

(2.14) with boundary conditions (2.15) have been solved using Runge-Kutta-Fehlberg fourth-fifth order method with Shooting technique. The non-linear ordinary differential equations (2.11)-(2.14) are of third order in  $f$  and second order in  $g, \theta$  &  $\phi$  and these coupled differential equations are first reduced into a

system of simultaneous ordinary equations. In order to solve this system of equations using Runge-Kutta-Fehlberg fourth-fifth method, one requires nine initial conditions. But only five initial conditions are known and however the values of  $f'(\eta), g(\eta), \theta(\eta), \phi(\eta)$  are known at  $\eta = \infty$ . These end conditions are used to obtain unknown initial condition  $\eta = 0$  using Shooting technique. In Shooting method the boundary value problem (BVP) is reduced to an initial value problem (IVP). The boundary value calculated is then matched with the real boundary value. Using trial and error or some scientific approach, one attempts to get as close to the boundary value as possible. The most essential step of this method is to choose the appropriate finite value for  $\eta$  at  $\infty$ .

We take infinity condition at a large but finite value of  $\eta$  where no considerable variation in velocity, temperature and so on occur. We run our bulk computations with the value at  $\eta_{max} = 5$ , which was sufficient to achieve the far field boundary conditions asymptotically for all values of the parameters considered.

To have a check on the accuracy of the numerical procedure used, first test computations for  $f''(0)$  and  $\theta'(0)$  are carried out for regular fluid (Newtonian fluid) for various values of stretching parameter  $A$  and melting parameter  $M$  and compared with the available published results of Bachok et al. [3] and Yacob et al. [44] in table 1 and they are found to be in excellent agreement.

#### 4. Results and Discussion

In this section, a representative set of graphical results for velocity, temperature and nanoparticle volume fraction as well as the local Nusselt number and skin friction coefficient are presented and discussed for various parametric conditions.

Figure 2 reveals the velocity and temperature distributions for different values of melting parameter. It is observed that for increasing the values of  $M$ , the velocity and temperature distributions decreases. This is because of increase in  $M$  will increase the intensity of melting which act as blowing boundary condition at the stretching surface hence tends to thicken the boundary layer. Figures 3 exhibit the effect of magnetic parameter on velocity and temperature profiles. The presence of a magnetic field in an electrically conducting fluid introduces a force called Lorentz force, which opposes the flow. This resistive force tends to slow down the flow, so that the effect of increasing  $Q$  is to decrease the velocity and also causes decreases in its temperature.

Figure 4 explains the effect of Radiation parameter on temperature and nanoparticle fraction profiles. It is observed that, the temperature profile decreases and nanoparticle fraction profiles increases for increasing the values of  $Nr$ . This is because, the large values correspond to an increased dominance of conduction over radiation thereby decreasing buoyancy force and thickness of the thermal boundary layer. Figures 5 exhibit the velocity and angular velocity profiles for variable values of material parameter ( $R$ ). The fluid velocity and angular velocity is found to be decreases with increasing the values of  $R$ . It is because increasing the material parameter leads to the increase in the total viscosity of the flow, which thus retards the flow.

Figure 6 presents typical profile for temperature  $\theta(\eta)$  and concentration  $\phi(\eta)$  for various values of Thermophoretic parameter ( $Nt$ ). It is observed that in both the cases an increase in the  $Nt$  leads to increase in fluid temperature and nanoparticle concentrations. This Thermophoresis serves to warm the boundary layer for low values of  $Pr$  and Lewis number ( $Le$ ). The effect of Brownian motion parameter ( $Nb$ ) on temperature and concentration are shown in figures 7. As expected, temperature in the boundary layer increases and the nanoparticle volume fraction decreases with the increase in  $Nb$ . This is because Brownian motion serves to warm the boundary layer and simultaneously exacerbates particle deposition away from the fluid regime or onto the surface, thereby accounting for the reduced concentration magnitudes.

Figure 8 indicates the effects of velocity and angular velocity profiles for  $n$ . From this, we observed that the velocity increases and angular velocity decreases for increasing the values of  $n$ . In figure 9 we exhibit the effect of  $A$  on velocity and angular velocity profiles. Both velocity and angular velocity profiles increases as the stretching ratio  $A = a/c$  increases. This is due to the fact

that a fixed value of  $a/c > 1$  implies increase in the straining motion near the stagnation-point region resulting in increased acceleration of the external stream. This leads to thinning of the boundary layer with increase in  $A$ . We noticed from the figure 10 that influence of stretching ratio  $A$  is to increase the temperature and concentration profile significantly.

The effect of Lewis number ( $Le$ ) on concentration profile are illustrated in figure 11. It is clearly observed that the nanoparticle volume fraction as well as its boundary-layer thickness increase considerably as the Lewis number  $Le$  increases. Figure 12 depicts the effect of  $Pr$  on temperature profiles respectively. In the presence of melting parameter, an increase in Prandtl number increases the temperature profiles and also from figure 13 we can see that the angular velocity increases near the plate and decreases far away from the plate for increasing values of  $Q$ .

The figures 14(a) and 14 (b) displays the nature of heat transfer coefficient against  $Nb$  for different values of  $Nt$ . Heat transfer increases for both Brownian motion parameter ( $Nb$ ) and thermophoresis parameter ( $Nt$ ). Similarly, the heat transfer decreases with  $Pr$  for different values of  $Nr$ . Figures 15(a) and 15(b) illustrate the variations of skin friction  $f''(0)$  versus material parameter  $R$  for different values of melting parameter ( $M$ ). One can be noticed that the skin friction decreases with an increase in the melting parameter ( $M$ ). Similarly, the variation of skin friction  $f''(0)$  versus stretching parameter  $A$  for different values of  $n$ . From this it is observed that, the skin friction increases with an increase in the parameter  $n$ .

#### 5. Conclusion

We have studied numerically the effect of melting on boundary layer stagnation flow of Micropolar Nanofluid over a liner stretching sheet in presence of radiation and applied magnetic field. The model used for the nanofluid is the model proposed by Buongiorno which studies the effects of Brownian motion and the thermophoresis. Solutions of system of coupled equations are obtained using a Shooting method program with a Runge-Kutta-Fehlberg-45 method. Comparison with previously published work was performed and the results were found to be in good agreement.

The main findings of the study are summarized as follows;

- The boundary layer thickness and the velocity are found to be increases as the melting parameter increases, but the reverse trend is true for both the magnetic and the radiation parameters.
- A boundary condition to account for melting was used at the interface between the solid and liquid phases.
- In the presence of a uniform magnetic field, increase in the strength of the applied magnetic field decelerated the fluid motion along the wall of the plate

and also causes decreases in its temperature inside the boundary layer.

- The magnitudes of the skin friction coefficient and the local Nusselt number increase with an increase in the melting process.
- Angular velocity increases near the plate and decreases far away from the plate for increasing values of  $\Omega$ .

#### Acknowledgement:

The authors gratefully acknowledge the reviewers for their constructive comments and valuable suggestions.

#### References

1. Awaludin. I.S., Weidman, P.D., and Ishak, A., 2016, "Stability analysis of stagnation-point flow over a stretching/shrinking sheet," AIP ADVANCES, 6, pp. 045308.
2. Ahmad, S., Rohni, A.M., and Pop, I., 2011, "Blasius and Sakia-dis problems in nanofluids, Acta. Mech., 218, pp. 195-204.
3. Bachok, N., Ishak, A., and Pop, I., 2010, "Melting heat transfer in boundary layer stagnation-point flow towards a stretching/shrinking sheet," Physics Letters A., 374, pp. 4075-4079.
4. Bachok, N., Ishak, A., Nazarand, R., and Pop, I., 2010, "Flow and heat transfer at a general three-dimensional stagnation point flow in a nanofluid," Physica B., 405, pp. 4914-4918.
5. Bachok, N., Ishak, A., and Pop, I., 2011, "Flow and heat transfer over a rotating porous disk in a nanofluid," Physica B, 406, pp. 1767-1772.
6. Buongiorno, J., 2006, "Convective transport in nanofluids," J. Heat Tran., 128, pp. 40-250.
7. Chamkha, A.J., Rashad, A.M., and Eisa Al-Meshaieci, 2011, "Melting effect on unsteady hydromagnetic flow of a nanofluid past a stretching sheet," International Journal of Chemical Reactor Engineering, 9, pp. 1-13.
8. Epstein, M., and Cho, D.H., 1976, "Melting heat transfer in steady laminar Flow over a flat plate," J. Heat transfer, 98(3), pp. 531-533.
9. Eringen, A.C., 1966, "Theory of micropolar fluids," J. Math Mech., 16, pp. 1-18.
10. E.Abu-Nada and Oztop, H.F., 2009, "Effect of inclination angle on natural convection in enclosures filled with Cu-water nanofluid," Int. J. Heat Fluid Flow, 30, pp. 669-678.
11. Goyal, M., and Bhargava, R., 2013, "Thermodiffusion effects on boundary layer flow of viscoelastic nanofluids over a stretching sheet with viscous dissipation and non-uniform heat source using hp-finite element method," Proceedings of the Institution of Mechanical Engineers, Part N: Journal of Nanoengineering and Nanosystems, 227(2), pp. 77-99.
12. Gorla, R.S.R., Chamkha. A., and Aloraier, A.K., 2011, "Melting heat transfer in a nanofluid flow past a permeable continuous moving surface," Journal of Naval Architecture and Marine Engineering, 2, pp. 83-92.
13. Hiemenz, K., 1911, "Die Grenzschicht an einem in den gleichformigen Flüssigkeitsstrom eingetauchtengeraden Kreiszyylinder," Dingler's Polytech J., 326(21), pp. 321-324.
14. Hayat, T., Muhammad, K., Farooq, M., and Alsaedi, A., 2016, "Melting heat transfer in stagnation point flow of carbon nanotubes towards variable thickness surface," AIP ADVANCES, 6, pp. 015214.
15. Hussain, T., Shehzad, S.A., Hayat, T., Alsaedi, A., and Al-Solamy, F., 2014, "Radiative hydromagnetic flow of Jeffrey nanofluid by an exponentially stretching sheet," PLoS ONE, 9(8), pp. e103719.
16. Hayat, T., Ashraf, M.B., Shehzad, S.A., and Bayomi, N.N., 2015, "Mixed convection flow of viscoelastic nanofluid over a stretching cylinder," J. Braz. Soc. Mech. Sci. Eng., 37(3), pp 849-859.
17. Hayat, T., and Farooq, M., 2014, "Melting heat transfer in the stagnation-point flow of Maxwell fluid with double-diffusive convection," International Journal of Numerical Methods for Heat & Fluid Flow, 24(3), pp. 760-774.
18. Ishak, A., Nazar, R., and Pop, I., 2009, "Dual solutions in mixed convection boundary layer flow of micropolar fluids," Communications in Nonlinear Science and Numerical Simulation, 14, pp. 1324-1333.
19. Jankowski, D.F., and Gersting, J.M., 1970, "Unsteady three-dimensional stagnation-point flow, AIAA Journal ,8 (1), pp. 187-188.
20. Khan, W.A., and Gorla, R.S.R., 2011, "Heat and mass transfer in non-Newtonian nanofluids over a non-isothermal stretching wall," Proceedings of the Institution of Mechanical Engineers, Part N: Journal of Nanoengineering and Nanosystems, 225(4), 155-163.
21. Khan, W.A., Uddin. M.J., and Ismail A. Md., 2012, "Effect of momentum slip on double-diffusive free convective boundary layer flow of a nanofluid past a convectively heated vertical plate," Proceedings of the Institution of Mechanical Engineers, Part N: Journal of Nanoengineering and Nanosystems, 226(3), pp. 99-109.
22. Kuznetsov, A.V., and Nield, D.A., 2010, "Natural convective boundary layer flow of a nanofluid past a vertical plate," Int. J. Thermal Sci., 49, pp. 243-247.
23. Khan, W.A., Khan, M., and Malik, R., 2014, "Three-Dimensional flow of an Oldroyd-B nanofluid towards stretching surface with heat generation/ absorption," PLoS ONE, 9(8), pp. e105107.

24. Krishnamurthy, M.R., Prasannakumara, B.C., Gireesha, B.J., and Gorla, R.S.R, 2016, "Effect of chemical reaction on MHD boundary layer flow and melting heat transfer of Williamson nanofluid in porous medium," *Engineering Science and Technology, an International Journal*, 19, pp. 53–61.
25. Mohanty, B., Mishra, S.R., and Pattanayak, H.B., 2015, "Numerical investigation on heat and mass transfer effect of micropolar fluid over a stretching sheet through porous media," *Alexandria Engineering Journal*, 54, pp. 223–232.
26. Muthamilselvan, M., Kandaswamy, P., and Lee, J., 2010, "Heat transfer enhancement of Copper-water nanofluids in a lid-driven enclosure," *Comm. Nonlinear Sci. Numer. Simulat.*, 15, pp. 1501-1510.
27. Mabood, F., and Das, K., 2016, "Melting heat transfer on hydromagnetic flow of a nanofluid over a stretching sheet with radiation and second-order slip," *Eur. Phys. J. Plus*, 131, pp. 3.
28. Malik, M.Y., Naseer, M., Nadeem, S., and Abdul Rehman, 2014, "The boundary layer flow of Cassonnanofluid over a vertical exponentially stretching cylinder," *Appl. Nanosci.*, 4, pp. 869–873.
29. Nadeem, S., RizwanUlHaq, and Khan, Z.H., 2014, "Numerical solution of non-Newtonian nanofluid flow over a stretching sheet," *ApplNanosci.*, 4, pp. 625–631.
30. Nadeem, S., Sadiq, M.A., Jung-il Choi, and Changhoon Lee, 2014, "Exponentially stagnation point flow of non-Newtonian nanofluid over an exponentially stretching surface," *Int. J. Non-linear Sci. Numer. Simul.*, 15(3–4), pp. 171–180.
31. Nadeem, S., and Hussain, S.T., 2014, "Flow and heat transfer analysis of Williamson nanofluid," *Appl. Nanosci.*, 4(8), pp. 1005–1012.
32. Roberts, L., 1958, "On the melting of a semi-infinite body of ice placed in a hot stream of air," *Journal of Fluid Mechanics*, 4, pp.505-528.
33. RizwanUlHaq, Nadeem, S., Khan, Z.H., and Okedayo, T.G., 2014, "Convective heat transfer and MHD effects on Cassonnanofluid flow over a shrinking sheet," *Cent. Eur. J. Phys.*, 12(12), pp. 862-871.
34. Ramesh, G.K., and Gireesha, B.J., 2014, "Influence of heat source/sink on a Maxwell fluid over a stretching surface with convective boundary condition in the presence of nanoparticles," *Ain Shams Engineering Journal*, 5, pp. 991–998.
35. Subhas M. Abel., and JayashreeSanamani, 2015, "Melting heat transfer in mhd boundary layer stagnation-point flow towards a stretching sheet with thermal radiation," *Materials Science & Engineering*, ISSN 2412-5954.
36. Singh, K., Singh, P., and Kumar, M., 2014, "Melting heat transfer in boundary layer stagnation point flow of micropolar fluid towards a porous stretching/shrinking surface," *National Conference on Synergetic Trends in engineering and Technology (STET-2014)*, *International Journal of Engineering and Technical Research*, ISSN: 2321-0869,
37. Shehzad, S.A., Hayat, T., Alsaedi, A., and Obid, M.A., 2014, "Nonlinear thermal radiation in three-dimensional flow of Jeffrey nanofluid: A model for solar energy," *Applied Mathematics and Computation*, 248, pp. 273–286.
38. Shehzad, S.A., Hayat, T., and Alsaedi, A., 2015, "MHD flow of Jeffrey nanofluid with convective boundary conditions," *J Braz. Soc. Mech. Sci. Eng.*, 37(3), pp 873–883.
39. Tiwari, R.K., and Das, M.K., 2007, "Heat transfer augmentation in a two-sided lid-driven differentially heated square cavity utilizing nanofluids," *Int. J. Heat Mass Tran.*, 50, pp. 2002-2018.
40. Talebi, F., Mahmoudi, A.H., and Shahi, M., 2010, "Numerical study of mixed convection flows in a square lid-driven cavity utilizing nanofluid," *International Communications in Heat and Mass transfer*, 37(1), pp. 79-90.
41. WilliamsIII, J.C., 1968, "Non steady stagnation-point flow," *AIAA Journal*, 6 (12), pp. 2417-2419.
42. Wang, C.Y., 2008, "Stagnation flow towards a shrinking sheet," *Int. J. Non-Linear Mech.*, 43, pp. 377–82.
43. Yang, K.T., 1958, "Unsteady laminar boundary layers in an incompressible stagnation flow," *Trans. ASME J. Appl. Mech.*, 25, pp. 421-427.
44. Yacob, N.A., Ishak, A., and Pop, I., 2011, "Melting heat transfer in boundary layer stagnation-point flow towards a stretching/shrinking sheet in a micropolar fluid," *Computers and Fluids*, 47, pp. 16-21.
45. Yacob, N.A., Ishak, A., and Pop, I., 2011, "Melting heat transfer in boundary layer stagnation-point flow towards a stretching/shrinking sheet in a micropolar fluid," *Computers and Fluids*, 47, pp. 16-21.
46. Yacob, N.A., Ishak, A., Pop, I., and Vajravelu, K., 2011, "Boundary layer flow past a stretching/shrinking surface beneath an external uniform shear flow with a convective surface boundary condition in a nanofluid," *Nanoscale Research Letters*, 6, pp. 314.
47. Zaimi, K., and Ishak, A., 2016, "Stagnation-point flow towards a stretching vertical sheet with slip effects," *Mathematics*, 4, pp. 27.

**Tables and Figures:**

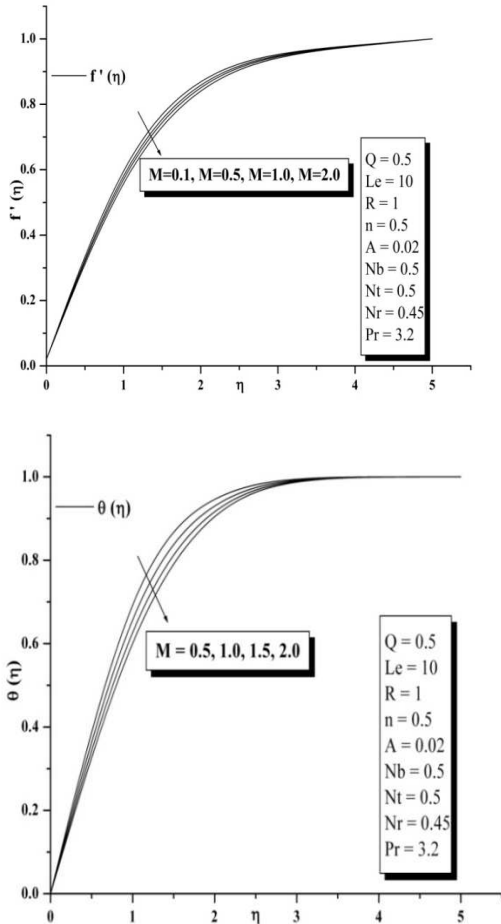


Figure 2: Effect of  $M$  on velocity and temperature profiles.

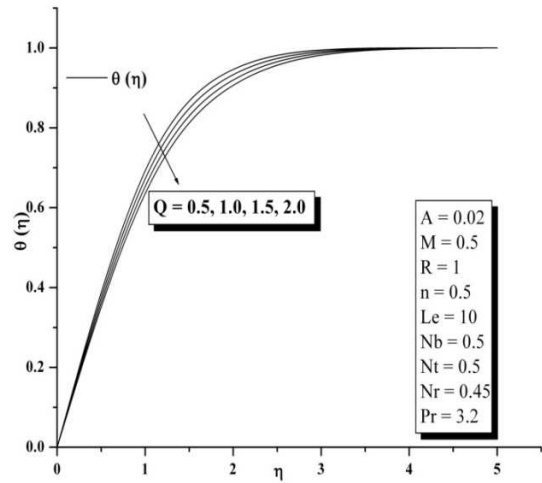
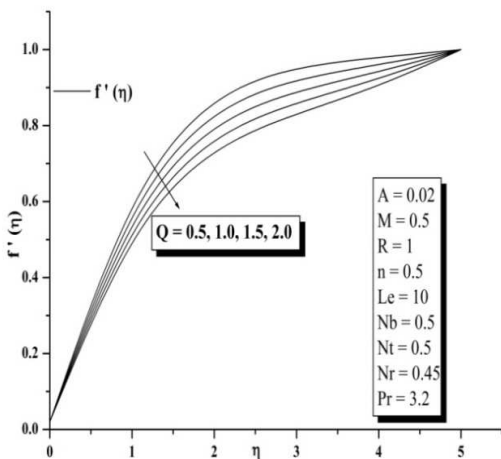


Figure 3: Effect of  $Q$  on velocity and temperature profiles.

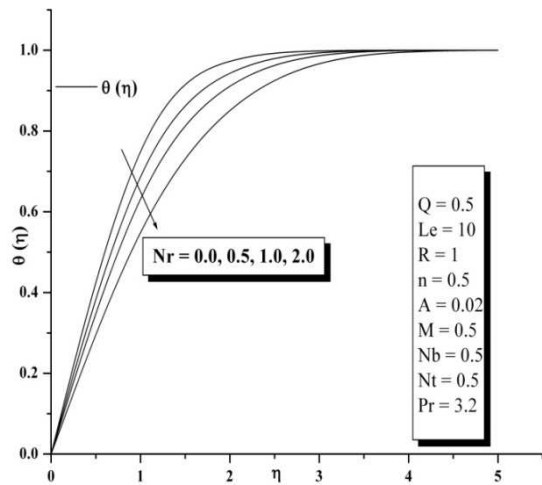
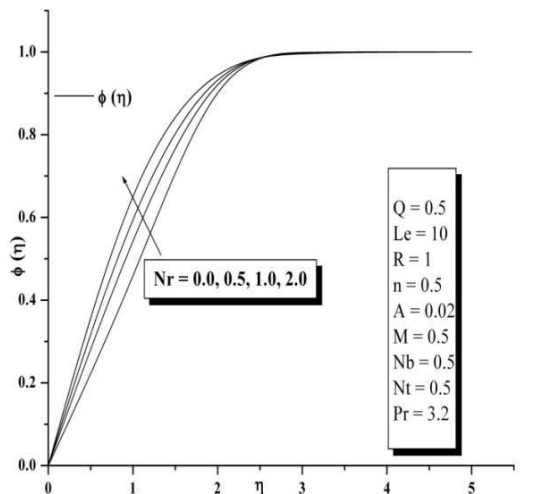


Figure 4: Effect of  $Nr$  on temperature and concentration profiles.





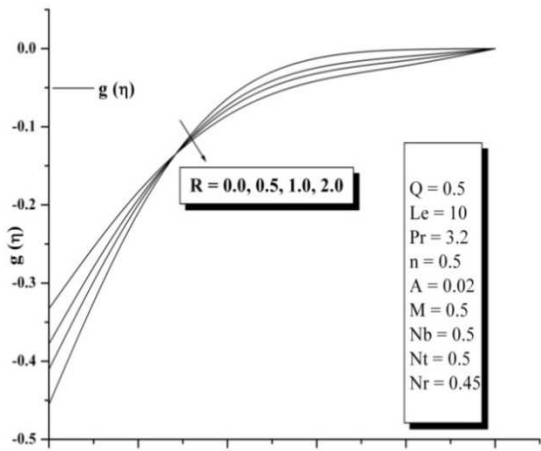
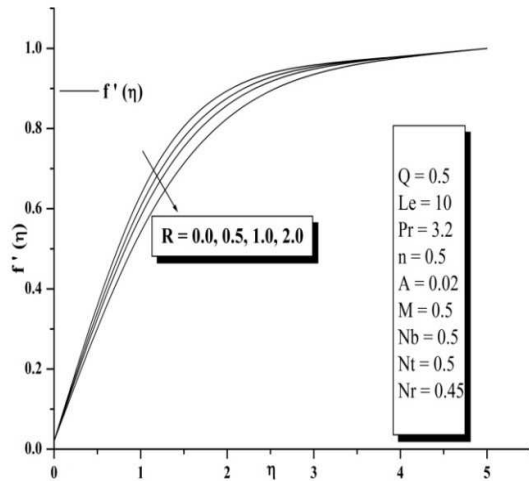


Figure 5: Effect of  $R$  on velocity and angular velocity profiles.

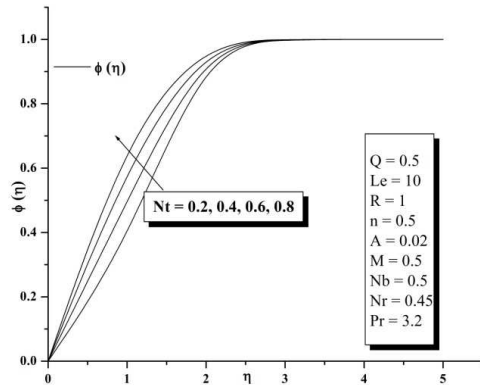
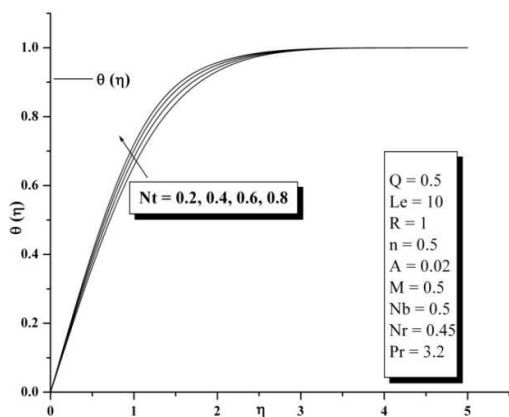


Figure 6: Effect of  $Nt$  on temperature and concentration profiles.

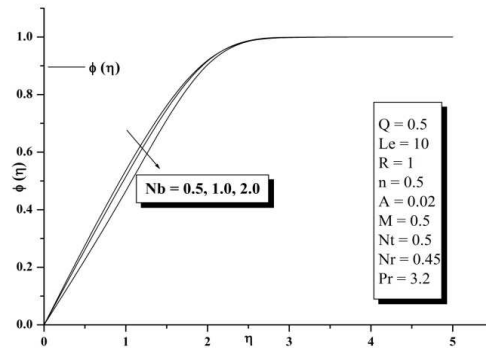
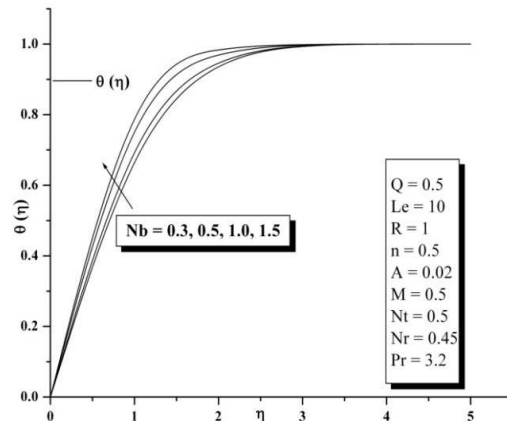


Figure 7: Effect of  $Nb$  on temperature and concentration profiles.

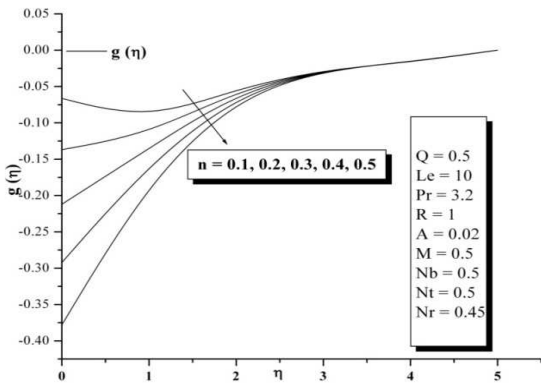
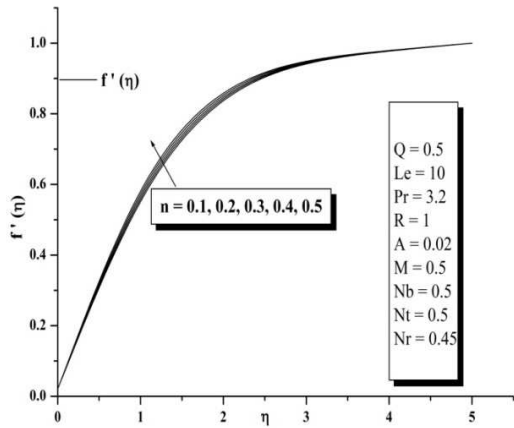


Figure 8: Effect of  $n$  on velocity and angular velocity profiles.

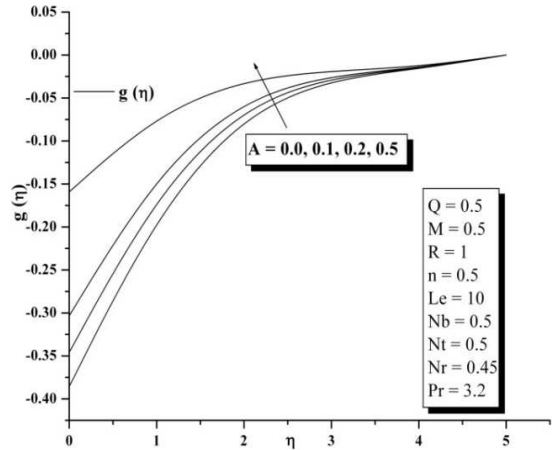
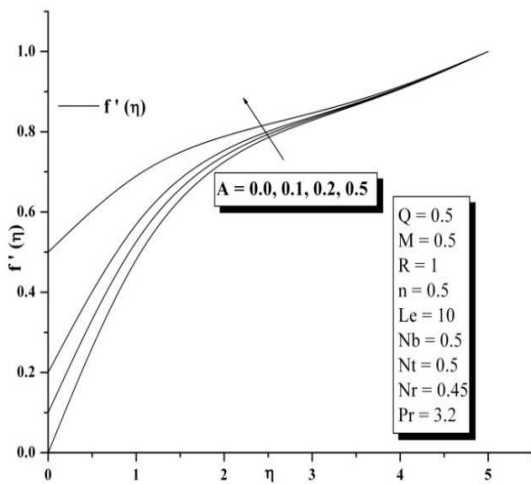


Figure 9: Effect of  $A$  on velocity and angular velocity profiles.

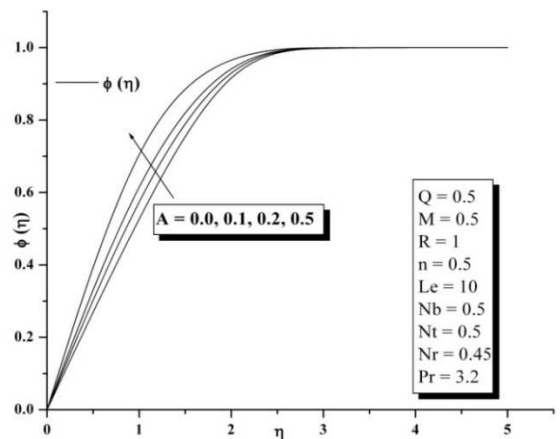
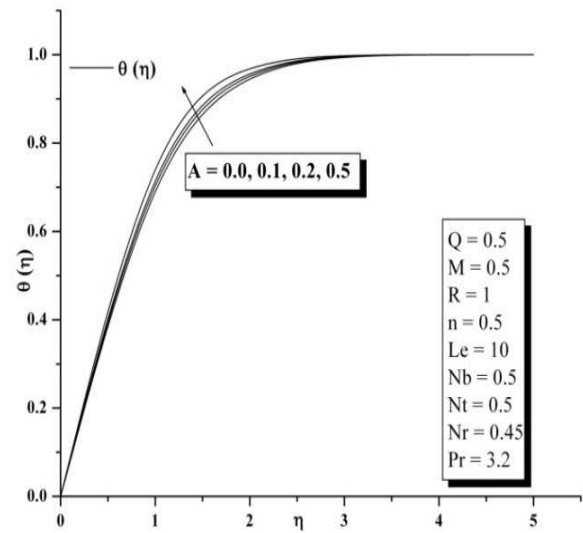


Figure 10: Effect of  $A$  on temperature and concentration profile.

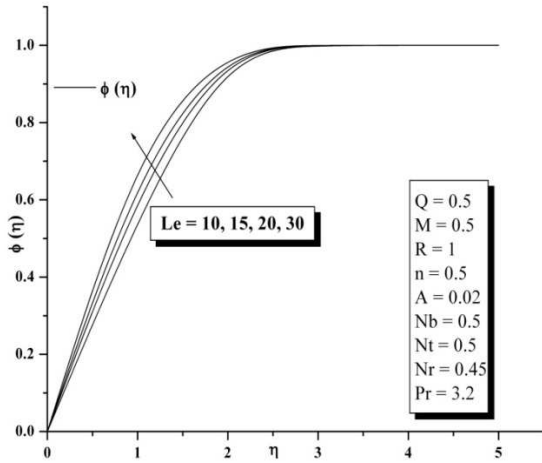


Figure 11: Effect of  $Le$  on concentration profiles

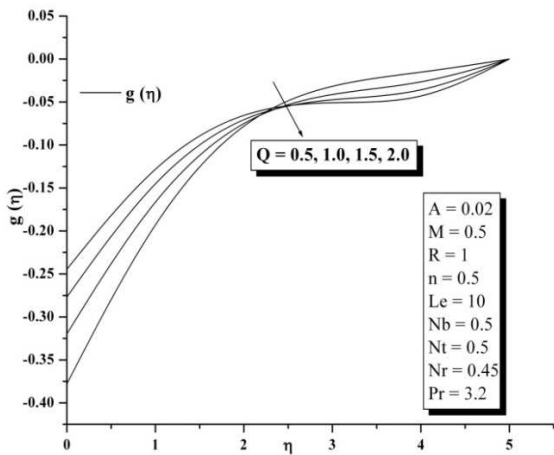


Figure 12: Effect of  $Q$  on angular velocity.

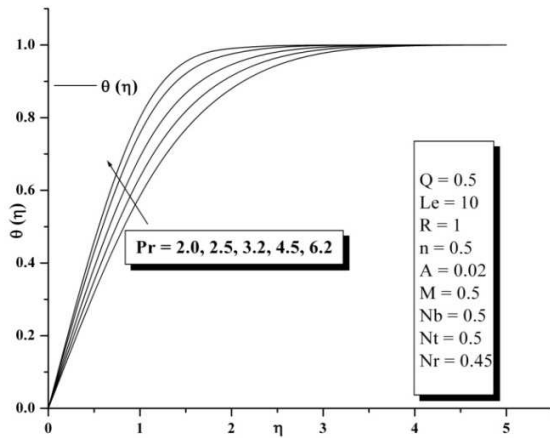


Figure 13: Effect of  $Pr$  on temperature profiles.

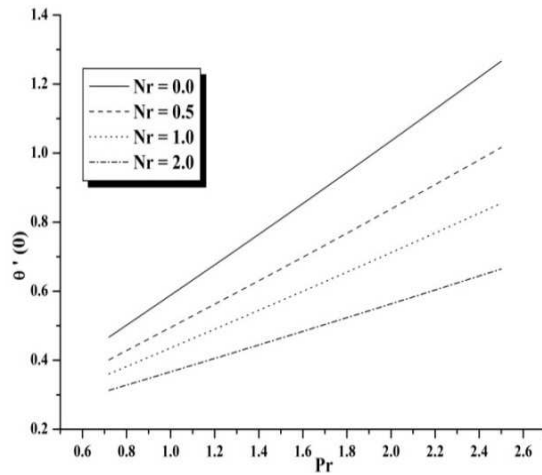
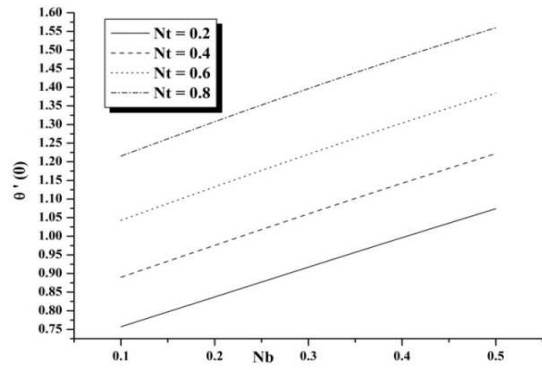
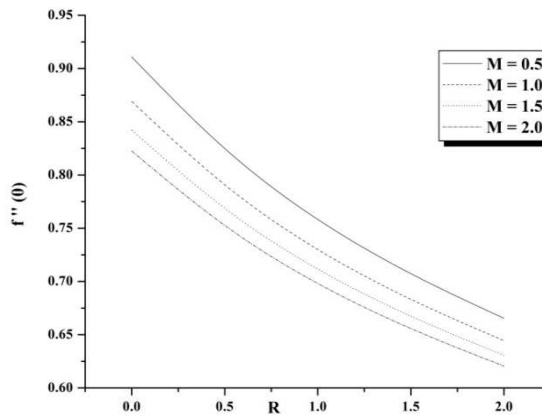


Figure 14 (a), (b): Variation of  $\theta'(0)$  with  $Nb$  for different with  $Nt$  and variation with  $Pr$  for different values of  $Nr$ .



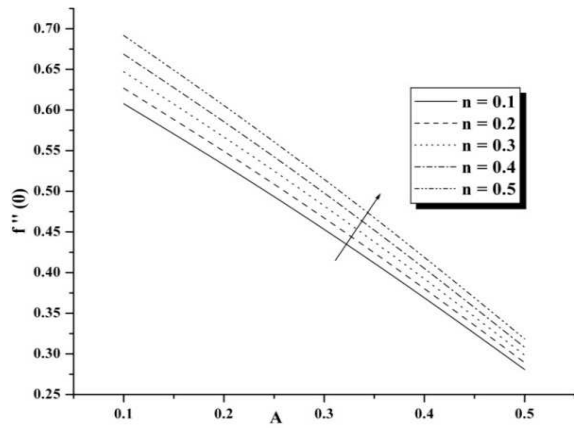


Figure 15(a), (b): Effect of skin friction coefficient with  $A$  for different values of  $n$  and with  $n$  for different values of  $A$

**Table 1:** Comparison of present values of  $f'''(0)$  and  $-\theta'(0)$  for different values of stretching parameter  $A$  and melting parameter  $M$ , when  $\beta, Ec, Q, R, N = 0$  and  $Pr = 1$ .

| parameter: |     | Eckert et al [3] |               | Yacob et al [44] |               | Present study |               |
|------------|-----|------------------|---------------|------------------|---------------|---------------|---------------|
| $A$        | $M$ | $f'''(0)$        | $-\theta'(0)$ | $f'''(0)$        | $-\theta'(0)$ | $f'''(0)$     | $-\theta'(0)$ |
| 0.0        | 0.0 | 1.23525876       |               | 1.2325877        | 0.570465      | 1.23258768    | 0.570469995   |
|            | 1.0 | 1.0370034        |               | 1.037003         | 0.361961      | 1.036997334   | 0.361913338   |
|            | 2.0 | 0.9468506        |               |                  |               | 0.946833343   | 0.273721264   |
| 0.5        | 3.0 | 0.891381         |               |                  |               | 0.89139121    | 0.223162584   |
|            | 0.0 | 0.7132949        |               | 0.713295         | 0.692064      | 0.713294966   | 0.692065815   |
|            | 1.0 | 0.5990895        |               | 0.59909          | 0.438971      | 0.599088513   | 0.438971285   |
| 1.0        | 2.0 | 0.5043333        |               |                  |               | 0.5047017449  | 0.331927254   |
|            | 3.0 | 0.5151721        |               |                  |               | 0.515166211   | 0.270616779   |
|            | 0.0 |                  | 0.7978846     |                  |               | 0.713294966   | 0.797884176   |
| 2.0        | 1.0 |                  | 0.5060545     |                  |               |               | 0.50605615    |
|            | 2.0 |                  | 0.3826383     |                  |               |               | 0.38264128    |
|            | 3.0 |                  | 0.3119564     |                  |               |               | 0.311960624   |
| 2.0        | 0.0 | -1.8873066       |               | -1.887307        | 0.979271      | -1.88730663   | 0.979271368   |
|            | 1.0 | -1.5804839       |               | -1.580483        | 0.621187      | -1.58048373   | 0.62118726    |
|            | 2.0 | -1.4427473       |               | -1.442747        |               | -1.4427467    | 0.469711948   |
|            | 3.0 | -1.3592105       |               |                  |               | -1.35920926   | 0.382950899   |